

Domain structures and quark potentials in SU(3) gauge theory

Seyed Mohsen Hosseini Nejad*

Faculty of Physics, Semnan University, P.O. Box 35131-19111, Semnan, Iran

We analyze the static potentials for various representations in SU(3) Yang-Mills theory within the framework of the domain model of center vortices. The influence of vortex interactions is investigated on the static potentials. We show that, by ad-hoc choosing the probability weights of the different vortex configurations contributing to the static potential, a phenomenologically satisfactory result for the different representations can be achieved. In particular including vacuum domains, a way to effectively parametrize vortex interactions, is crucial in obtaining an (almost) everywhere convex potential when interpolating between the short distances and the asymptotic regimes.

PACS. 11.15.Ha, 12.38.Aw, 12.38.Lg, 12.39.Pn

I. INTRODUCTION

Understanding quark confinement and the dynamical mechanism behind it is a big challenge in QCD. The interaction between static quark sources at small separations is dominated by one-gluon exchange and the potential is Coulomb-like. At intermediate distances, quark confinement arises referring to the color electric flux-tube formation and linear potentials. In this range of distances, the string tensions for different representations are qualitatively in agreement with Casimir scaling [1–3]. At asymptotic distances, the string tensions depend only on the N -ality of the representations [4]. In addition, the quark potential must be everywhere convex and without concavity [5]. Numerical simulations [6–11] and infrared models [12–19] have indicated that center vortices [20–25] which are quantized magnetic flux tubes could account for the quark confinement via the area law of the Wilson loop. Furthermore, numerical simulations have shown that the center vortices could also account for spontaneous chiral symmetry breaking [26–32].

The thick center vortex model [12, 13] is a phenomenological model trying to understand the color confinement in terms of the interaction of the Wilson loops with the center vortices. However, the potentials induced by center vortices for some representations show unphysical concavity when interpolating between the short distances and the asymptotic regimes. For removing the concavity, in Ref. [16], the vortex profile is allowed to fluctuate.

In this paper, this artifact is studied through analyzing vortex interactions. We represent various forms of the center vortex picture of confinement for static quark potentials in different representations of SU(3). In the thick center vortex model, we investigate the Yang-Mills vacuum of the SU(3) gauge theory including two types of center vortices. In some literatures, two types of vortices may be regarded as the same type of vortex but with magnetic flux pointing in opposite directions. Without this constraint, we study the behavior of these center vortices on static potentials in this analytical model. Although interactions of both types of center vortices with sufficiently large Wilson loops are the same, their interactions with medium size Wilson loops are different. Besides, Casimir scaling and N -ality regimes for some representations do not connect smoothly and some kind of unexpected concavity occurs in the model which explicitly disagrees with lattice results. In Refs. [13, 33, 34], a domain structure is assumed in the vacuum for G(2) and SU(N) gauge theories. The total magnetic flux through each domain corresponds to a center element of $\mathbb{Z}(N)$ subgroup. In the framework of the domain model of center vortices, we analyze the domain structures with a fixed vortex profile for removing concavity and improving Casimir scaling especially for higher representations of the SU(3) gauge group. Interactions between two types of vortices are discussed using a dual analogy to the type II superconductivity where it seems that two vortices repel each other while the vortex-antivortex interaction is attractive. Moreover, we argue that the same interactions may be confirmed by the model. We show that interactions between two types of center vortices may deform them to the configurations with the lowest magnitude of center fluxes where there are appeared vortices of type one as well as vacuum domains on the vacuum. We show that ad-hoc choosing the probability weights of the domain structures is crucial in obtaining an (almost) everywhere convex potential.

In Sec. II, we analyze the static potentials in various representations and their ratios induced by center vortices in SU(3) gauge theory within the framework of the thick center vortex model. We investigate the contributions of center

*Electronic address: smhosseininejad@ut.ac.ir

vortices and the vortex interactions in the potentials in Sec. III. Then, in Sec. IV the confinement mechanism in the background of center vortices would be reformulated for removing concavity and improving the Casimir scaling. We summarize the main points of our study in Sec. V.

II. STATIC POTENTIALS INDUCED BY TWO TYPES OF SU(3) CENTER VORTICES

Any non-Abelian SU(N) gauge theory of confinement should explain some features of the confining force which can be verified in lattice simulations. If one neglects dynamical quarks in the vacuum in the first approximation, the static quark potential of nonperturbative regime has distinct behavior in two ranges of interquark distances. At intermediate distances, from the onset of the confinement to the onset of color screening, the quark potential is expected to be linearly rising and the string tension of the quark potential for the representation r is approximately proportional to C_r , the eigenvalue of the quadratic Casimir operator for the representation r , i.e. $\sigma_r \approx \frac{C_r}{C_F} \sigma_F$ where F denotes the fundamental representation [1–3]. When the energy between quarks suffices, a gluon pair is created in the vacuum and Casimir scaling breaks down and is replaced by an N -ality dependent law [4]. Therefore, at asymptotic distances, the quark potential depends on the N -ality k_r of the representation i.e. $\sigma_r = \sigma(k_r)$. The string tension $\sigma(k_r)$ corresponds to the lowest dimensional representation of SU(N) with N -ality k_r . In addition, the lattice results [5] show that the static quark potential must be everywhere convex i.e.

$$\frac{dV}{dr} > 0 \quad \text{and} \quad \frac{d^2V}{dr^2} \leq 0. \quad (2.1)$$

Therefore, it is crucial to obtain a convex potential without any concavity when interpolating between the short distances and the asymptotic regimes.

Any model of the quark confinement should be able to explain these features for the potentials between static quarks. The thick center vortex model has been fairly successful in describing the mechanism of confinement in QCD [12]. However there are still some shortcomings within the model which is at the focus of this article. In this model, the vacuum is assumed to be filled with center vortices. In SU(N) gauge group, there are $N - 1$ types of center vortices corresponding to the nontrivial center elements of $z_n = \exp(i2\pi n/N) \in \mathbb{Z}(N)$ enumerated by the value $n = 1, \dots, N - 1$. The effect of a thick center vortex on a planar Wilson loop is to multiply the loop by a group factor

$$W_r(C) \rightarrow G_r(\alpha_C^n(x))W_r(C), \quad (2.2)$$

where the function $G_r(\alpha_C^n(x)) = 1/d_r \text{Tr} \exp[i\vec{\alpha}_C^n \vec{H}]$, d_r is the dimension of the representation, and $\{H_i\}$ is the set of generators from the Cartan subalgebra. The function $\alpha_C^n(x)$ denotes the vortex profile and this angle depends on both the Wilson loop C and the position of the vortex center x . If the center vortex is all contained within the Wilson loop $\exp[i\vec{\alpha}_C^n \vec{H}] = (z_n)^{k_r} \mathbb{I}$ where k_r is the N -ality of representation r . Using this constraint, the maximum value of the angle α_{max}^n could be calculated. If the center vortex is outside the loop $\exp[i\vec{\alpha}_C^n \vec{H}] = \mathbb{I}$ and therefore it has no effect on the loop. The quark potential induced by the center vortices is as follows [12]:

$$V_r(R) = - \sum_x \ln(1 - \sum_{n=1}^{N-1} f_n [1 - \text{Re} G_r(\vec{\alpha}_C^n(x))]), \quad (2.3)$$

where the parameter f_n determines the probability that any given plaquette is pierced by an n th center vortex. An ansatz for the angle $\vec{\alpha}_C^n$ was introduced by Greensite *et al.* [13]. Each center vortex with square cross section $A_v = L_v \times L_v$ contains small independently fluctuating subregions of area $l^2 \ll A_v$ which l is a short correlation length. The only constraint is that the total magnetic fluxes of the subregions must correspond to a center element of the gauge group. This square ansatz is as follows:

$$\vec{\alpha}_C^n(x) \cdot \vec{\alpha}_C^n(x) = \frac{A_v}{2\mu} \left[\frac{A}{A_v} - \frac{A^2}{A_v^2} \right] + \left(\alpha_{max}^n \frac{A}{A_v} \right)^2, \quad (2.4)$$

where A is the cross section of the center vortex overlapping with the minimal area of the Wilson loop and μ is a free parameter.

Now, we apply the model to the SU(3) gauge group with center $\mathbb{Z}(3)$. The homotopy group

$$\Pi_1[SU(3)/\mathbb{Z}(3)] = \mathbb{Z}(3), \quad (2.5)$$

implies that the SU(3) gauge theory has center vortices corresponding to the nontrivial center elements. In SU(3) case, there are two types of center vortices corresponding to the nontrivial center elements $z_1 = \exp(i2\pi/3)$ and

$z_2 = \exp(i4\pi/3)$. In some literatures, vortices of type z_1 and type z_2 have phase factors which could be considered complex conjugates of one another ($z_1 = z_2^*$) and therefore two vortices may be regarded as the same type of vortex but with magnetic flux pointing in opposite directions. Without this constraint, vortex fluxes of two types of center vortices are different and we analyze the behavior of these center vortices on static potentials. Using Eq. (2.3), the static potential induced by center vortices in $SU(3)$ gauge group is as follows:

$$V_r(R) = - \sum_{x=-L_v/2}^{L_v/2+R} \ln[(1 - f_1 - f_2) + f_1 \text{Re}G_r(\alpha_C^1(x)) + f_2 \text{Re}G_r(\alpha_C^2(x))], \quad (2.6)$$

where f_1, f_2 are the probabilities that any given plaquette is pierced by z_1 and z_2 center vortices, respectively. The square ansatz given in Eq. (2.4) for the angles corresponding to the center vortices for all representations are:

$$(\alpha_C^1(x))^2 = \frac{A_v}{2\mu} \left[\frac{A}{A_v} - \frac{A^2}{A_v^2} \right] + \left(\frac{4\pi}{\sqrt{3}} \frac{A}{A_v} \right)^2, \quad (\alpha_C^2(x))^2 = \frac{A_v}{2\mu} \left[\frac{A}{A_v} - \frac{A^2}{A_v^2} \right] + \left(\frac{8\pi}{\sqrt{3}} \frac{A}{A_v} \right)^2. \quad (2.7)$$

The free parameters L_v, f_1, f_2 , and $L_v^2/(2\mu)$ are chosen to be 100, 0.01, 0.01, and 4, respectively. The correlation length is taken $l = 1$ and therefore the potentials are linear from the beginning ($R = l$). Now, we study the static potentials of the lowest representations in $SU(3)$ gauge theory. Figure 1 shows the Young diagrams as well as N -ality k of the representations.

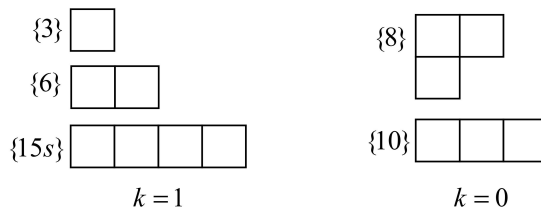


FIG. 1: The Young diagrams for the lowest representations of $SU(3)$. The N -ality k of the representations are shown below the diagrams. The label s means the representation is symmetric.

Figure 2 a) plots the static potentials $V_r(R)$ induced by two types of center vortices for these representations in the range $R \in [0, 100]$. At intermediate distances, the potentials are linear in the range $R \in [0, 20]$. The potential ratios $V_{\{r\}}(R)/V_{\{3\}}(R)$ for the various representation r are shown in Fig. 2 b). These ratios start out at the Casimir ratios:

$$\frac{C_{\{6\}}}{C_{\{3\}}} = 2.5, \quad \frac{C_{\{8\}}}{C_{\{3\}}} = 2.25, \quad \frac{C_{\{10\}}}{C_{\{3\}}} = 4.5, \quad \frac{C_{\{15s\}}}{C_{\{3\}}} = 7. \quad (2.8)$$

In the range $R \in [0, 20]$, the potential ratios for the various representations drop slowly from Casimir ratios. However, the deviations from the exact Casimir scaling are much greater for higher representations.

At large distances, the static potentials agree with N -ality where gluons can bind to the initial sources and string tensions of the representations are reduced to the lowest-dimensional representation with the same N -ality. In particular, zero N -ality representations are screened. For example, an adjoint charge combining with a gluon can form a color-singlet, $[\{8\} \otimes \{8\} = \{1\} \oplus \dots]$. More dynamical gluons might be required for screening of higher representations with zero N -ality. Nonzero N -ality representations through combining with gluons are transformed into the lowest order representations. For example, a tensor product of $[\{6\} \otimes \{8\} = \{3\} \oplus \dots]$ shows that the slope of the potential for the representation $\{6\}$ must be the same as the one for the representation $\{3\}$.

As a result, the model leads to Casimir scaling at the intermediate distances and exhibits N -ality at the asymptotic regimes, in agreement with lattice calculations. But these two regimes for several representations do not connect smoothly and some kind of unexpected concavity occurs in the model which explicitly disagrees with lattice results.

In the next section, for reducing the concavity of some representations, we argue about the behavior of two types of center vortices on the vacuum through analyzing their effects on the Wilson loops.

III. CENTER VORTEX CONTRIBUTIONS IN THE POTENTIALS

For analyzing the concavity of the potentials in $SU(3)$ gauge group, we study the potentials induced by two types of center vortices in more details. As shown in Fig. 2 a), the concavity is appeared for several representations such

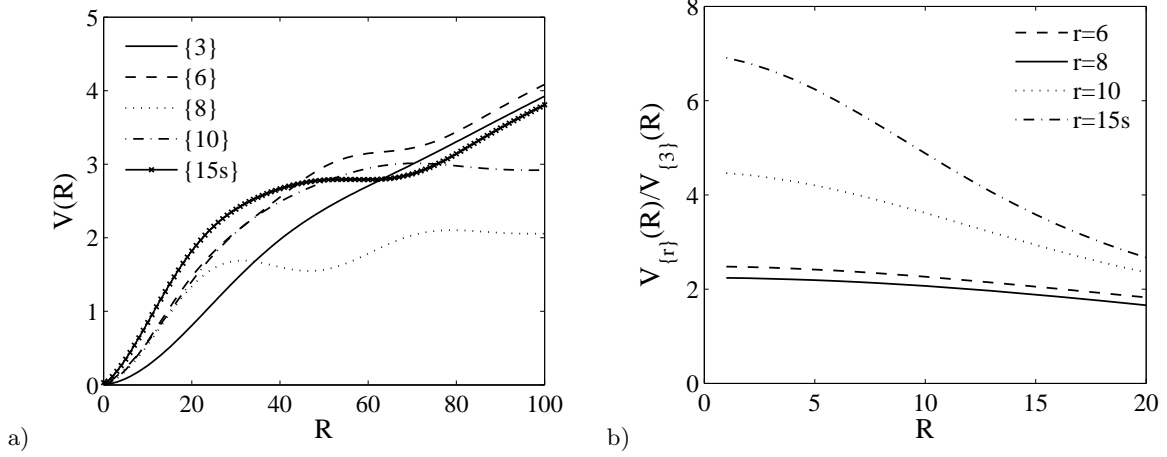


FIG. 2: a) The static potentials using both types of center vortices for various representations of $SU(3)$. The concavity is appeared for several representations. b) Potential ratios $V_{\{r\}}(R)/V_{\{3\}}(R)$ at the intermediate distances. The ratios start from the Casimir ratios and violate slowly from the Casimir ratios in this regime. However, the deviations from the exact Casimir scaling are much greater for higher representations. The free parameters are $L_v = 100$, $f_1 = f_2 = 0.01$, and $L_v^2/(2\mu) = 4$.

as the adjoint representation. Figure 3 depicts the potentials induced by two types of center vortices individually for the adjoint representation. The concavity is appeared in the static potential induced by center vortices of type two while there is no this artifact in the potential obtained by center vortices of type one.

The behavior of a group factor gives some information about the details of its potential. The functions of the group factors for the lowest representations of $SU(3)$ can be found in the Appendix. Now, we analyze the group factors corresponding to two types of center vortices for the adjoint representation close to the concavity regime (about $R = 60$). The time-like legs of the Wilson loop are located at $x = 0$ and $x = 60$. When the center vortex overlaps the minimal area of the Wilson loop, it affects the Wilson loop. As shown in Fig. 4 a), z_1 vortex group factor changes smoothly with a minimum value around any time-like leg ($x = 0, 60$) while for the z_2 vortex group factor a wavy character with equal large sizes of maxima and minima is observed the neighborhood of any these regimes. Therefore, the large fluctuations of the group factor around any time-like leg lead to the concavity behavior in the potentials. As shown in Fig. 4 b), at large distances ($R = 100$) governed with the N -ality, the group factors for both types of center vortices in the adjoint representation interpolate from 1, when the vortex core is located entirely within the Wilson loop, to 1, when the core is entirely outside the loop. As shown in Fig. 4, a fluctuation with a minimum is appeared around each time-like leg for the z_1 vortex group factor in the adjoint representation while two of these fluctuations occur around each time-like leg for the z_2 vortex group factor. Since z_2 vortices are characterized by the center element $z_2 = z_1^2$, there is periodicity in the z_2 vortex group factor and its potential compared with those of the z_1 vortex.

Furthermore, Fig. 5 a) depicts the group factors corresponding to two types of center vortices for the medium size Wilson loop with $R = 15$ for the fundamental representation and the ones for the large size loop with $R = 100$ are plotted in Fig. 5 b). As shown, the z_1 vortex group factor in the fundamental representation changes smoothly around each time-like leg and therefore one could expect that the group factor of $z_2 = z_1^2$ changes smoothly the neighborhood of each time-like leg.

At large distances, the group factors for both types of center vortices in the fundamental representation interpolate from -0.5 , when the vortex core is located entirely within the Wilson loop, to 1, when the core is entirely outside the loop. As shown in Fig. 5 a), decreasing the size of the Wilson loop ($R = 15$), the minimum value of the z_1 vortex group factor is increased while the one of the z_2 vortex group factor is close to center vortex value (-0.5). The value of the z_2 vortex group factor for the medium size Wilson loops is about center vortex value which is related to N -ality regimes. Therefore, we expect that the z_2 vortices break down somewhat the Casimir scaling at intermediate distances. Figure 6 plots the potential ratios induced by center vortices for the range $R \in [0, 20]$. As shown, the contributions of two types of the center vortices are compared. For various representations, the potential ratios obtained from the z_1 vortices which start from the Casimir ratios drop slower than those induced by both types of vortices.

For detailed analysis of two types of vortices, we note to the interactions between vortices. The QCD vacuum could be described in terms of a Landau-Ginzburg model of a dual superconductor where it follows the electric flux tube formation and confinement of the electric charge. A dual superconductor is like type II superconductors but the roles of the electric and magnetic fields, and electric and magnetic charges, have been interchanged [36, 37]. Properties of

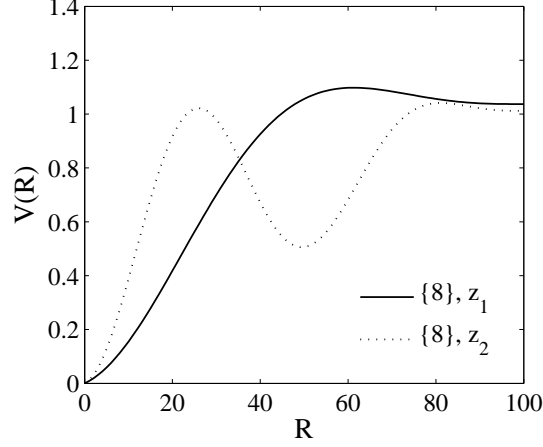


FIG. 3: The static potentials induced by two types of center vortices individually for the adjoint representation. The concavity is observed for the potential induced by z_2 center vortices while there is no this artifact in the potential obtained by z_1 center vortices. The free parameters are $L_v = 100$, $f_1 = f_2 = 0.01$, and $L_v^2/(2\mu) = 4$.

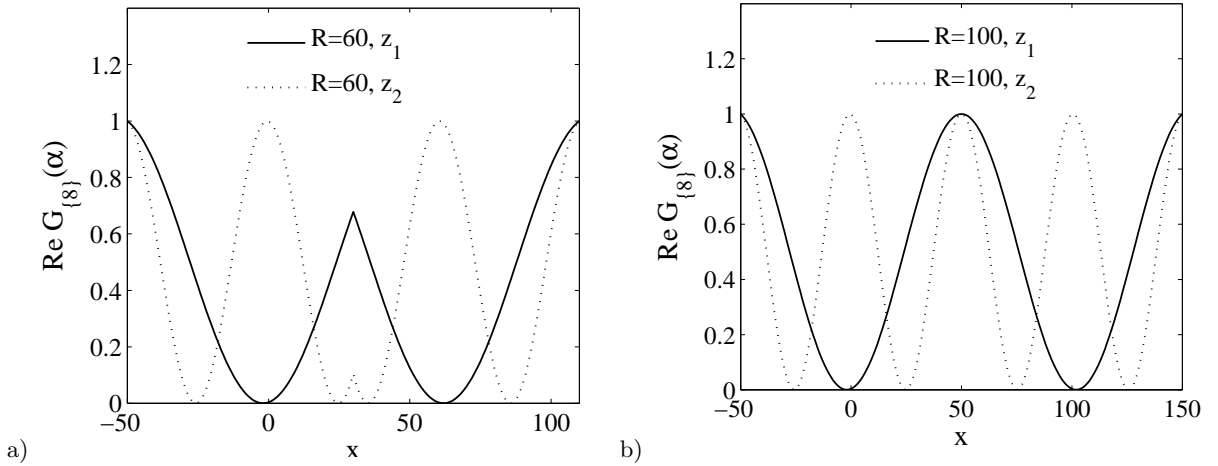


FIG. 4: a) The group factors $\text{Re} G_{\{8\}}(\alpha)$ of the two types of center vortices versus x corresponding to Fig. 3 at $R = 60$, close to the concavity regime. The fluctuations of the z_2 vortex group factor with equal large sizes of maxima and minima around any time-like leg lead to concavity behavior in the potentials. b) The same as a) but for the large size Wilson loop with $R = 100$. In agreement with the color screening in the large regime for the adjoint representation, the group factors for both types of center vortices when the vortex core is located entirely within the Wilson loop is equal to 1. The free parameters are $L_v = 100$ and $L_v^2/(2\mu) = 4$.

superconductors are often described in terms of the superconducting coherence length ξ and the London magnetic field penetration depth λ . The Ginzburg-Landau parameter $\kappa = \lambda/\xi$ of the type-II superconductor is larger than $1/\sqrt{2}$. In the type II superconductors, there are vortices as the magnetic flux lines as well as the magnetic fluxes pointing in opposite directions of vortices (antivortices). The interaction between vortices is repulsive while the vortex-antivortex interaction is attractive [38, 39]. Furthermore, one may find the same interactions between vortices in the model which is discussed in the next section. Now, using these results, the vacuum is argued in SU(3) case, filled with z_2 vortices as well as z_1 vortices. Such z_2 vortices are characterized by the center element $z_2 = z_1^2$. The z_2 vortex is constructed of two z_1 vortices with the same flux orientations and therefore these z_1 vortices according to the interactions in the type-II superconductor repel each other. One may conclude that z_2 vortices do not make a stable configuration and one should consider each of z_1 vortices within the z_2 vortices as a single vortex in the model. In addition, only vortices with the smallest magnitude of center flux have substantial probability [12]. In fact, this probability for the z_2 vortex should be less than the one for the z_1 vortex. In previous section, we considered the general case that all possible f_n are included and therefore the concavity is appeared for several representations. Now, we assume only z_1 vortices in

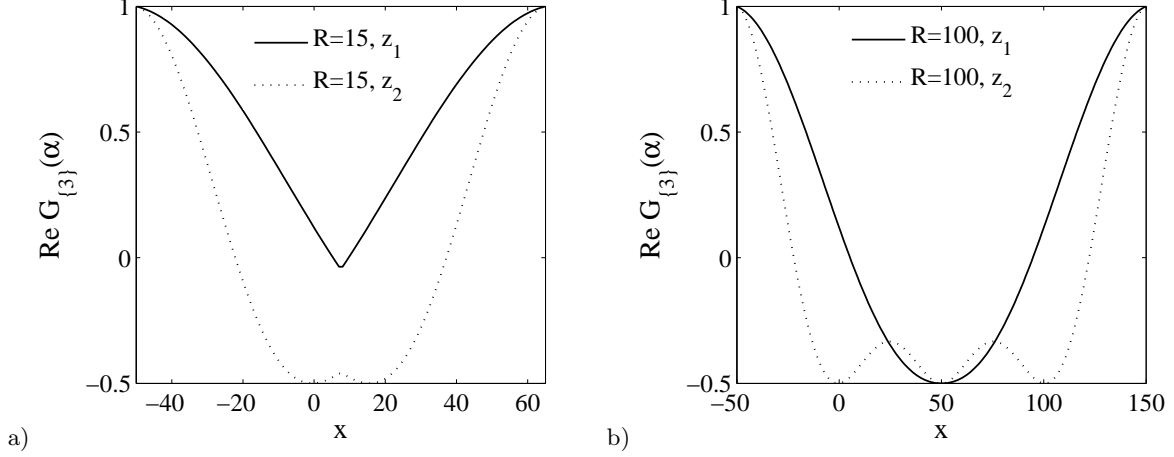


FIG. 5: a) The group factors $\text{Re}G_{\{3\}}(\alpha)$ of the two types of center vortices versus x for the fundamental representation in the intermediate distance with $R = 15$. b) the same as a) but for the asymptotic distance with $R = 100$. The group factors for both types of center vortices when the vortex core is located entirely within the Wilson loop is equal to -0.5 . Decreasing the size of the loop, the minimum value of the z_1 vortex group factor is increased and becomes close to trivial value while the one of the z_2 vortex group factor is close to center vortex value (-0.5). The free parameters are $L_v = 100$ and $L_v^2/(2\mu) = 4$.

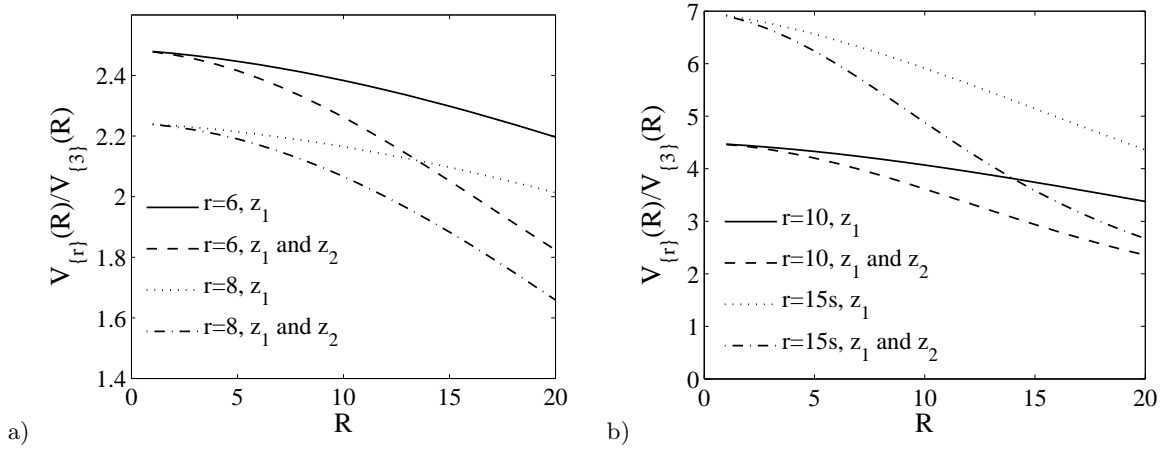


FIG. 6: The potential ratios of $V_{\{r\}}(R)/V_{\{3\}}(R)$ induced by center vortices for the various representations. Upper curve of any representation shows the contribution of the z_1 vortices which violates more slowly from the Casimir ratio compared with the contribution of the z_1 vortices plus the z_2 vortices. For all representations, the ratios induced by the z_1 vortices agree better with Casimir scaling compared with the ratios induced by z_2 vortices. The free parameters are $L_v = 100$, $f_1 = f_2 = 0.01$, and $L_v^2/(2\mu) = 4$.

the vacuum. Figure 7 shows the potentials for the various representations in the range $R \in [0, 100]$.

Although, using only z_1 vortices, two Casimir scaling and N -ality distances are smoothly connected for some representations, the concavity occurs for higher representations especially $\{15s\}$. Indeed, this concavity is observed independent of the ansatz for the angle [16].

The next step, the confinement mechanism in the background of center vortices would be reformulated for removing this concavity and we discuss two types of $SU(3)$ center vortices in more details.

IV. VACUUM DOMAINS AND REMOVING THE CONCAVITY OF THE POTENTIALS

The QCD vacuum is a dual analogy to the type II superconductivity. As argued, it seems that two vortices repel each other while the vortex-antivortex interaction is attractive. On the one hand, two z_1 vortices within the z_2 vortex repel each other and one could observe them as the single vortices. On the other hand, in addition to two types of

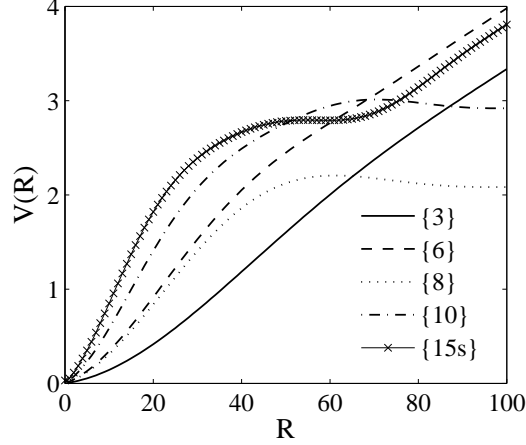


FIG. 7: The static potentials using z_1 center vortices for the various representations of $SU(3)$. Although the concavity is removed somewhat this artifact stays for higher presentations especially $\{15s\}$. The free parameters are $L_v = 100$, $f_1 = 0.01$, and $L_v^2/(2\mu) = 4$.

center vortices, there are their antivortices corresponding to complex conjugates of center elements on the vacuum. Therefore, z_2 and z_1^* vortex configurations attract each other and they would merge forming $z_2 z_1^* = z_1^2 z_1^* = z_1 z_0$ where $z_1 z_1^*$ is equal to the identity element $z_0 = 1$. In Refs. [13, 33, 34], vacuum domains corresponding to the identity element are also allowed in the model. The Yang-Mills vacuum has a domain structure where there are domains of the center-vortex type and of the vacuum type. Therefore, we observe that attractions between z_2 and z_1^* vortices are forming z_1 vortices as well as vacuum domains. One could apply the same argument for z_2^* and z_1 vortex configurations. The domain structures can be readily generalized to $SU(4)$ and beyond. For example, in $SU(4)$, there are non-trivial center elements $z_1 = \exp(i\pi/2)$, $z_2 = z_1^2$, and $z_3 = z_1^3$. The attractions between vortices and anti-vortices in $SU(4)$ may form center vortices as well as vacuum domains. Using Eq. (2.3), the static potential induced by center vortices as well as the vacuum domains is:

$$V_r(R) = - \sum_{x=-L_v/2}^{L_v/2+R} \ln(1 - \sum_{n=0}^{N-1} f_n [1 - \text{Re} G_r(\vec{\alpha}_C^n(x))]), \quad (4.1)$$

where the contribution of the vacuum domains ($n = 0$) is added. If a vacuum domain is all contained within the Wilson loop $\exp[i\vec{\alpha}_C^0 \vec{H}] = z_0 \mathbb{I}$. The total magnetic flux through a vacuum domain is zero value and therefore the square ansatz given in Eq. (2.4) for the angle of vacuum domain for all representations is

$$(\alpha_C^0(x))^2 = \frac{A_v}{2\mu} \left[\frac{A}{A_v} - \frac{A^2}{A_v^2} \right]. \quad (4.2)$$

Now, to understand the interactions between two types of $SU(3)$ center vortices, we study the static potentials in the fundamental representation. Figure 8 shows the static potentials induced by vortex configurations in the fundamental representation at large distances where the ansatz of the vortex profile has no role in the potentials. Each configuration is appeared in the plane of the Wilson loop with the probability $f_n = 0.01$. We assume that there are z_1 vortex as well as z_1^* antivortex on the vacuum. Adding z_1 vortex to the vortex configurations may lead either to $z_2 = z_1^2$ and z_1^* vortex configurations or to z_1 and $z_0 = z_1^* z_1$ vortex configurations. In other words, it is interesting to observe that this z_1 vortex is attracted by which one of the initial vortices, z_1 vortex or z_1^* antivortex. One expects that the ensemble of the vortex configurations leads to a minimum energy. The potential energy induced by z_1^* and z_2 vortex configurations is more than the one induced by z_1 and z_0 vortex configurations. It seems that for minimizing the energy z_2 and z_1^* attract each other and deform to z_1 and z_0 vortex configurations. The extra negative energy of the potential induced by z_1 and z_0 vortex configurations compared with the one induced by z_1^* and z_2 vortex configurations may be interpreted as an attraction energy between z_1 and z_1^* vortices and repulsion between two z_1 vortices. Therefore, two magnetic vortex fluxes with the same orientation may repel each other while those with the opposite orientation attract each other. It seems that the model also confirms the interactions between vortices in the type II superconductivity. In addition, we studied the interaction between vortices in the model based

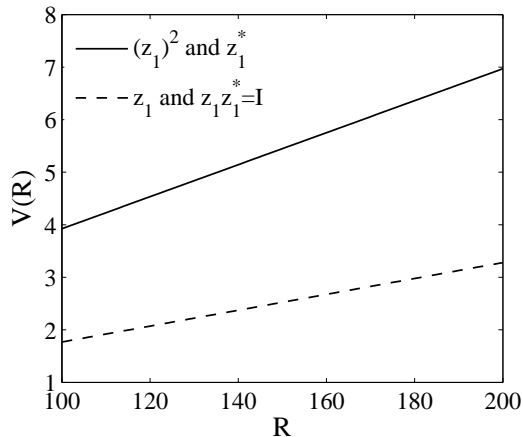


FIG. 8: The static potential induced by z_1 and z_0 vortex configurations is compared with the one induced by z_1^* and z_2 vortex configurations in the fundamental representation at large distances. It seems that for minimizing the energy z_2 and z_1^* attract each other and deform to z_1 and z_0 vortex configurations. For each configuration, the free parameters are $f_n = 0.01$, $L_v = 100$, and $L_v^2/(2\mu) = 4$.

on energetics in Refs. [34, 35] approving the same results for the interactions. It seems that the attractions between two types of center vortices produce vortices of type $n = 1$ and vacuum domains. It is possible that only vortices with the smallest magnitude of center flux have substantial probability to find the midpoints of them at any given location [12]. It seems that z_2 vortices, which its magnitude of center flux is twice the one of z_1 vortices, interacting with z_1 vortices are decomposed to the configurations with the lowest magnitude of center fluxes, i.e., z_1 vortices and vacuum domains.

Therefore, in SU(3) case using Eq. (4.1), the static potential induced by z_1 vortices and vacuum domains is

$$V_r(R) = - \sum_{x=-L_v/2}^{L_v/2+R} \ln[(1 - f_0 - 2f_1) + f_0 \text{Re}G_r(\alpha_C^0(x)) + 2f_1 \text{Re}G_r(\alpha_C^1(x))], \quad (4.3)$$

where the vortices of type $n = 2$ is substituted with those of type $n = 1$ and vacuum domains. f_0, f_1 are the probabilities that any given plaquette is pierced by vacuum domains and z_1 vortices, respectively. In Fig. 9, the static potential for the representation $\{15s\}$ which has shown the worst concavity is plotted. On the vacuum, there are z_1 vortices with the fixed probability $f_1 = 0.01$ but the probability f_0 of vacuum domains is gradually increased from zero to 0.05. As shown, the concavity could almost be removed by appearing the vacuum domains in the vacuum. The concavity for the higher representation $\{27\}$ is also eliminated. Therefore, the satisfactory result can be achieved by ad-hoc choosing the probability weights of the different vortex configurations. In particular including vacuum domains, a way to effectively parametrize vortex interactions, is crucial in obtaining an (almost) everywhere convex potential.

To check the details of the static potential in the representation $\{15s\}$, we analyze its group factors. Figure 10 a) depicts the group factors corresponding to z_1 vortices and vacuum domains for the medium size Wilson loop close to concavity regime (about $R = 70$) for the representation $\{15s\}$ and those for the large size loop are plotted in Fig. 10 b). As shown in Fig. 10 a), for the z_1 vortex group factor, a wavy character with a large amplitude appears around to any time-like leg ($x = 0, 70$). The same behavior occurs for the z_2 vortex group factor in the adjoint representation and therefore the concavity is appeared in its potential. Increasing large fluctuations of the group factor leads to the concavity behavior in the potentials. But, the vacuum domain group factor changes smoothly (small fluctuations) close to trivial value 1 around any time-like leg. Therefore the concavity of the potential could be removed by including the vacuum domain contribution to the potential. As shown in Fig. 10 b), the group factor for z_1 vortices in the representation $\{15s\}$ at large distances ($R = 100$), like the one of the fundamental representation, interpolates from -0.5 , when the vortex core is located entirely within the Wilson loop, to 1, when the core is entirely outside the loop. Also, in the same interval, when the core of the vacuum domain is located entirely within the loop, the group factor reaches to the trivial value 1. Besides, as show in Ref. [34], the vacuum domains could enhance the Casimir scaling at the intermediate distances.

As a result, small fluctuations of the group factor close to the trivial value, which occur because of the interactions between center vortices, could remove concavity in the static potentials and also improve the Casimir scaling at the

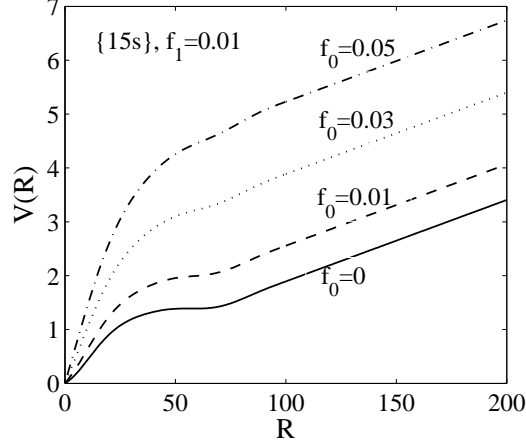


FIG. 9: The static potential for the representation $\{15s\}$. On the vacuum, there are z_1 vortices with the fixed probability $f_1 = 0.01$ while the probability f_0 of vacuum domains is gradually increased. The concavity could almost be removed by appearing the vacuum domains, a way to effectively parametrize vortex interactions. The free parameters are $L_v = 100$ and $L_v^2/(2\mu) = 4$.

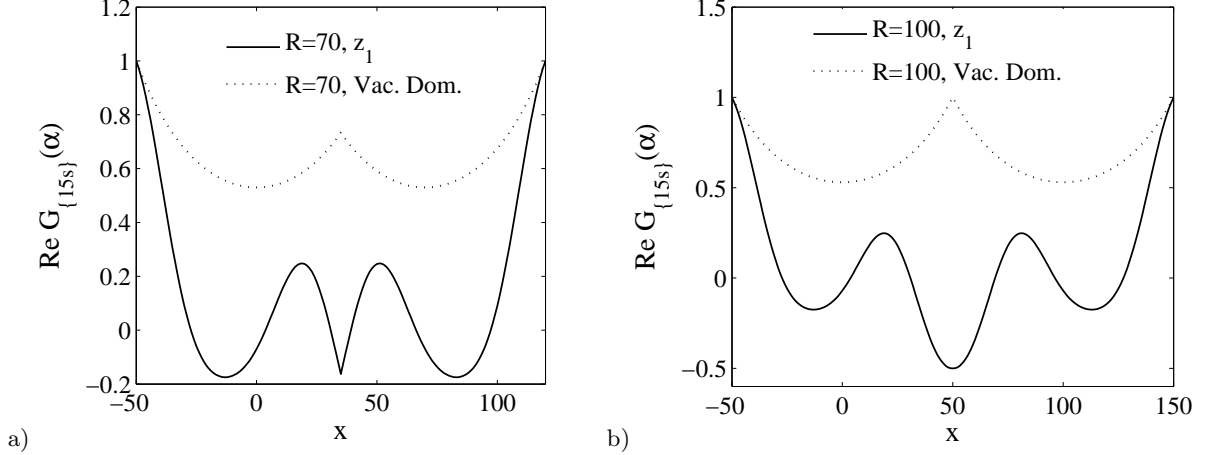


FIG. 10: a) The group factors $\text{Re } G_{\{15s\}}(\alpha)$ of the z_1 vortices and vacuum domains versus x at $R = 70$ corresponding to Fig. 9, close to the concavity regime. The fluctuations of the z_1 vortex group factor with equal large sizes of maxima and minima around any time-like leg lead to the concavity behavior in the potentials. The vacuum domain group factor changes smoothly close to the trivial value 1 around any time-like leg removing the concavity in the potential. b) The same as a) but for the large size Wilson loop with $R = 100$. Since the N -ality of the representation $\{15s\}$ is the same as the one of the fundamental representation, the z_1 vortex group factor like the one of the fundamental representation interpolates from -0.5 , when the vortex core is located entirely within the Wilson loop, to 1, when the core is entirely outside the loop. Also, in the same interval, when the core of vacuum domain is located entirely within the loop, the group factor reaches to the trivial value 1. The free parameters are $L_v = 100$ and $L_v^2/(2\mu) = 4$.

intermediate regime. But the large fluctuations of the group factor could create the concavity in the static potentials and break down the Casimir scaling at the intermediate regime.

In Fig. 11 a), the potentials $V_r(R)$ induced by z_1 vortices and vacuum domains for the various representations for the range $R \in [0, 200]$ are plotted and the potential ratios are shown in Fig. 11 b). Therefore, the satisfactory potentials for the different representations can be achieved by ad-hoc choosing the probability weights of the different vortex configurations. In particular including the vacuum domains, a way to effectively parametrize vortex interactions, is crucial in obtaining an (almost) everywhere convex potential when interpolating between the short distances and the asymptotic regimes. In addition, the potential ratios starting out at the Casimir ratios at intermediate distances drop very slowly from the exact Casimir scaling for all representations, especially for the higher representations. Therefore, the convex potentials in agreement with Casimir scaling at intermediate regimes with a fixed vortex profile could be

obtained, if one includes the contribution of vortex interactions in the static potentials.

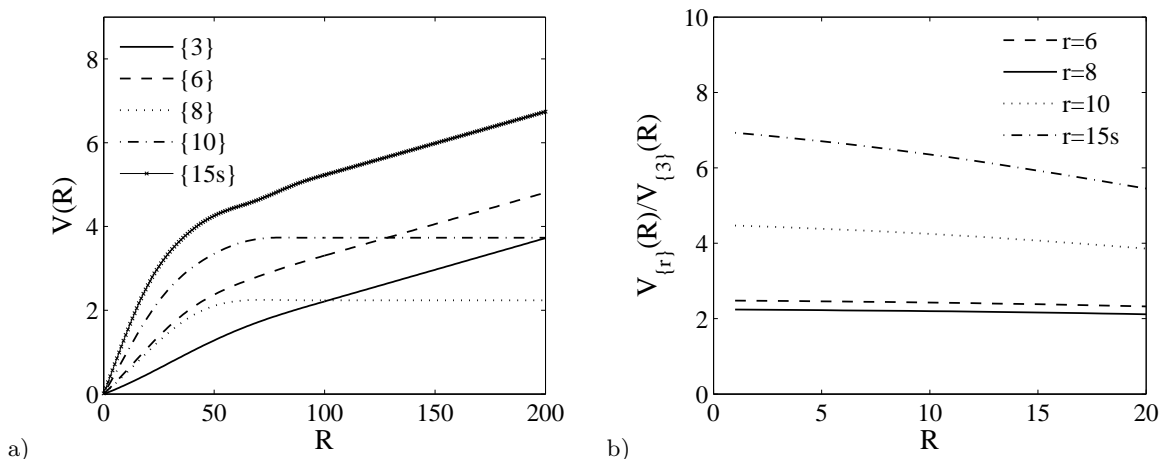


FIG. 11: a) The static potentials using both z_1 center vortices and vacuum domains for the various representations of $SU(3)$. The Casimir scaling and N -ality regimes connect naturally to each other without almost any concavity. b) Potential ratios $V_{\{r\}}(R)/V_{\{3\}}(R)$ at the intermediate distances. These potentials agree with Casimir scaling better than those obtained from both types of vortices, especially for the higher representations. The free parameters are $L_v = 100$, $f_0 = 0.05$, $2f_1 = 0.01$, and $L_v^2/(2\mu) = 4$.

Furthermore, when the properties of vortices in $d = 2$ dimensions and $\mathbb{Z}(N)$ models were being worked out, it was found that a real-space renormalization group approach to the $\mathbb{Z}(N)$ models reproduced the correct change in critical behavior at $N = 4$ if vacancies were included. In fact, it was found that the vacancy fugacity mimicked the vortex fugacity, and was a relevant variable in the disordered phase. In the framework of the real-space renormalization group approach [40–42], analyzing the convexity could be interesting and we will focus on this idea in the future works.

V. CONCLUSION

The static potentials in various representations depend on basic properties. At the intermediate regime, the potentials are governed by Casimir scaling while this feature breaks down in the asymptotic regime and is replaced by the N -ality dependent law. These two regimes should be connected smoothly to each other without any concavity. In this paper, we analyze the static potentials in $SU(3)$ Yang-Mills theory within the framework of the domain model of center vortices where there are two types of vortices. The two types of vortices may be regarded as the same type of vortex with magnetic flux pointing in opposite directions. Without this constraint, we study the behavior of these center vortices on static potentials. The interactions of both types of center vortices with large size Wilson loops are the same but their interactions with the medium size Wilson loops are different. The potentials induced by both vortex types show concave behavior for several representations. In addition, the potential ratios induced by z_1 vortices starting out at the Casimir ratios at intermediate distances drop slower than those of z_2 vortices. Analyzing the interactions between two types of center vortices, the confinement mechanism of center vortices is reformulated for removing the concavity of the potentials and also improving the Casimir scaling at the intermediate regimes. The QCD vacuum is a dual analogy to the type II superconductivity where it seems that two vortices repel each other while the vortex-antivortex interaction is attractive. We show that the model may also confirm the same interactions between vortices based on energetics. On the one hand, z_2 vortices are characterized by the center element $z_2 = z_1^2$ and two z_1 vortices within the z_2 vortex may repel each other and one could observe them as the single vortices. However using only z_1 vortices, this concavity would still remain for some higher representations. On the other hand, in addition to two types of center vortices, there are their antivortices on the vacuum. We show, like superconductivity, that z_2 and z_1^* vortex configurations may attract each other and therefore they would merge forming $z_2 z_1^* = z_1 z_0$ where z_0 is equal to the identity element. We observe that attractions between z_2 and z_1^* vortices are forming z_1 vortices as well as vacuum domains. Therefore, z_2 vortices, which its magnitude of center flux is twice the one of z_1 vortices, within the interactions with the z_1 vortices may be decomposed to the configurations with the lowest magnitude of center fluxes. As a result, the vacuum instead of z_1 and z_2 vortices is filled with z_1 vortices and vacuum domains. We show that by ad-hoc choosing the probability weights of the different vortex configurations, satisfactory result for

the static potentials can be achieved. In particular including the vacuum domains, a way to effectively parametrize vortex interactions, is crucial in obtaining the convex potentials in agreement with Casimir scaling at intermediate regimes.

Appendix A: Group factors of the representations

The Cartan generators for the representation r within the group factors of the static potential given in Eq. (4.1) can be calculated using the tensor method. One can obtain the real part of the group factors for all center domains in several representations as:

$$\text{Re}G_{\{3\}}(\alpha^n) = \frac{1}{3}[2\cos(\frac{\alpha^n}{2\sqrt{3}}) + \cos(\frac{\alpha^n}{\sqrt{3}})], \quad (\text{A1})$$

$$\text{Re}G_{\{6\}}(\alpha^n) = \frac{1}{6}[2\cos(\frac{\alpha^n}{2\sqrt{3}}) + 3\cos(\frac{\alpha^n}{\sqrt{3}}) + \cos(\frac{2\alpha^n}{\sqrt{3}})], \quad (\text{A2})$$

$$\text{Re}G_{\{8\}}(\alpha^n) = \frac{1}{8}[4 + 4\cos(\frac{3\alpha^n}{2\sqrt{3}})], \quad (\text{A3})$$

$$\text{Re}G_{\{10\}}(\alpha^n) = \frac{1}{10}[3 + 6\cos(\frac{3\alpha^n}{2\sqrt{3}}) + \cos(\frac{6\alpha^n}{2\sqrt{3}})], \quad (\text{A4})$$

$$\text{Re}G_{\{15_s\}}(\alpha^n) = \frac{1}{15}[4\cos(\frac{\alpha^n}{2\sqrt{3}}) + 3\cos(\frac{\alpha^n}{\sqrt{3}}) + 5\cos(\frac{2\alpha^n}{\sqrt{3}}) + 2\cos(\frac{5\alpha^n}{2\sqrt{3}}) + \cos(\frac{4\alpha^n}{\sqrt{3}})]. \quad (\text{A5})$$

-
- [1] C. Piccioni, *Casimir scaling in SU(2) lattice gauge theory*, Phys. Rev. D **73**, 114509 (2006).
 - [2] S. Deldar, *Static SU(3) potentials for sources in various representations*, Phys. Rev. D **62**, 034509 (2000).
 - [3] G. S. Bali, *Casimir scaling of SU(3) static potentials*, Phys. Rev. D **62**, 114503 (2000).
 - [4] S. Kratochvila and P. de Forcrand, *Observing string breaking with Wilson loops*, Nucl. Phys. B **671** (2003) 103.
 - [5] C. Bachas, *Convexity of the Quarkonium Potential*, Phys. Rev. D **33** (1986) 2723.
 - [6] L. Del Debbio, M. Faber, J. Greensite and S. Olejnik, *Center dominance and Z(2) vortices in SU(2) lattice gauge theory*, Phys. Rev. D **55** (1997) 2298.
 - [7] K. Langfeld, H. Reinhardt and O. Tennert, *Confinement and scaling of the vortex vacuum of SU(2) lattice gauge theory*, Phys. Lett. B **419** (1998) 317.
 - [8] L. Del Debbio, M. Faber, J. Greensite and S. Olejnik, *Center dominance, center vortices, and confinement*, hep-lat/9708023.
 - [9] K. Langfeld, O. Tennert, M. Engelhardt and H. Reinhardt, *Center vortices of Yang-Mills theory at finite temperatures*, Phys. Lett. B **452** (1999) 301.
 - [10] M. Engelhardt, K. Langfeld, H. Reinhardt and O. Tennert, *Deconfinement in SU(2) Yang-Mills theory as a center vortex percolation transition*, Phys. Rev. D **61** (2000) 054504.
 - [11] T. G. Kovacs and E. T. Tomboulis, *Vortices and confinement at weak coupling*, Phys. Rev. D **57** (1998) 4054.
 - [12] M. Faber, J. Greensite and S. Olejnik, *Casimir scaling from center vortices: Towards an understanding of the adjoint string tension*, Phys. Rev. D **57** (1998) 2603.
 - [13] J. Greensite, K. Langfeld, S. Olejnik, H. Reinhardt and T. Tok, *Color Screening, Casimir Scaling, and Domain Structure in G(2) and SU(N) Gauge Theories*, Phys. Rev. D **75** (2007) 034501.
 - [14] M. Engelhardt and H. Reinhardt, *Center vortex model for the infrared sector of Yang-Mills theory: Confinement and deconfinement*, Nucl. Phys. B **585** (2000) 591.
 - [15] M. Engelhardt, M. Quandt and H. Reinhardt, *Center vortex model for the infrared sector of SU(3) Yang-Mills theory: Confinement and deconfinement*, Nucl. Phys. B **685** (2004) 227.
 - [16] S. Deldar and S. Rafibakhsh, *Removing the concavity of the thick center vortex potentials by fluctuating the vortex profile*, Phys. Rev. D **81** (2010) 054501.
 - [17] S. Deldar, H. Lookzadeh and S. M. Hosseini Nejad, *Confinement in G(2) Gauge Theories Using Thick Center Vortex Model and domain structures*, Phys. Rev. D **85** (2012) 054501.
 - [18] S. Deldar and S. Rafibakhsh, *Short distance potential and the thick center vortex model*, Phys. Rev. D **80** (2009) 054508.

- [19] S. M. Hosseini Nejad and S. Deldar, *Role of the $SU(2)$ and $SU(3)$ subgroups in observing confinement in the $G(2)$ gauge group*, Phys. Rev. D **89** (2014) no.1, 014510.
- [20] G. 't Hooft, *On the Phase Transition Towards Permanent Quark Confinement*, Nucl. Phys. B **138** (1978) 1.
- [21] P. Vinciarelli, *Fluxon Solutions in Nonabelian Gauge Models*, Phys. Lett. **78B** (1978) 485.
- [22] T. Yoneya, *$Z(N)$ Topological Excitations in Yang-Mills Theories: Duality and Confinement*, Nucl. Phys. B **144** (1978) 195.
- [23] J. M. Cornwall, *Quark Confinement and Vortices in Massive Gauge Invariant QCD*, Nucl. Phys. B **157** (1979) 392.
- [24] G. Mack and V. B. Petkova, *Comparison of Lattice Gauge Theories with Gauge Groups $Z(2)$ and $SU(2)$* , Annals Phys. **123** (1979) 442.
- [25] H. B. Nielsen and P. Olesen, *A Quantum Liquid Model for the QCD Vacuum: Gauge and Rotational Invariance of Domained and Quantized Homogeneous Color Fields*, Nucl. Phys. B **160** (1979) 380.
- [26] P. de Forcrand and M. D'Elia, *On the relevance of center vortices to QCD*, Phys. Rev. Lett. **82** (1999) 4582.
- [27] M. Engelhardt, *Center vortex model for the infrared sector of Yang-Mills theory: Quenched Dirac spectrum and chiral condensate*, Nucl. Phys. B **638** (2002) 81.
- [28] R. Höllwieser, M. Faber, J. Greensite, U. M. Heller and S. Olejnik, *Center Vortices and the Dirac Spectrum*, Phys. Rev. D **78** (2008) 054508.
- [29] P. O. Bowman, K. Langfeld, D. B. Leinweber, A. Sternbeck, L. von Smekal and A. G. Williams, *Role of center vortices in chiral symmetry breaking in $SU(3)$ gauge theory*, Phys. Rev. D **84**, 034501 (2011).
- [30] S. M. Hosseini Nejad and M. Faber, *Colorful vortex intersections in $SU(2)$ lattice gauge theory and their influences on chiral properties*, JHEP **1709** (2017) 068.
- [31] R. Höllwieser, T. Schweigler, M. Faber and U. M. Heller, *Center Vortices and Chiral Symmetry Breaking in $SU(2)$ Lattice Gauge Theory*, Phys. Rev. D **88** (2013) 114505.
- [32] S. M. Hosseini Nejad, *Combining the color structures and intersection points of thick center vortices and low-lying Dirac modes*, Phys. Rev. D **97** (2018) no.5, 054516.
- [33] L. Lipták and Š. Olejník, *Casimir scaling in G_2 lattice gauge theory*, Phys. Rev. D **78** (2008) 074501.
- [34] S. M. Hosseini Nejad and S. Deldar, *Contributions of the center vortices and vacuum domain in potentials between static sources*, JHEP **1503** (2015) 016.
- [35] S. M. Hosseini Nejad and S. Deldar, *Correlations between Abelian Monopoles and center vortices*, Nucl. Phys. B **917**, 272 (2017).
- [36] G. 't Hooft, *High energy physics, in Gauge theories with unified weak, electromagnetic, and strong interactions*, edited by A. Zichichi (EPS International Conference, Palermo, 1975).
- [37] S. Mandelstam, *Vortices and quark confinement in non-abelian gauge theories*, Phys. Reports **23C**, 245–249 (1976).
- [38] L. Kramer, *Thermodynamic Behavior of Type-II Superconductors with Small kappa near the Lower Critical Field*, Phys. Rev. B **3**, 3821 (1971).
- [39] Andrey Chaves, F. M. Peeters, G. A. Farias, M. Milošević, *Vortex-vortex interaction in bulk superconductors: Ginzburg-Landau theory*, Phys. Rev. B **83**, 109905 (2011).
- [40] B. Nienhuis, E. K. Riedel and M. Schick, *Variational renormalisation-group approach to the q-state Potts model in two dimensions*, J. of Phys. A: Math. and Gen., **13**, 2 (1980).
- [41] F. L. Buessen, D. Roscher, S. Diehl, S. Trebst, *Functional renormalization group approach to $SU(N)$ Heisenberg models: Real-space renormalization group at arbitrary N* , Phys. Rev. B **97**, 064415 (2018).
- [42] L. Canet, B. Delamotte, D. Mouhanna, J. Vidal, *Nonperturbative renormalization group approach to the Ising model: A Derivative expansion at order ∂^4* , Phys. Rev. B **68**, 064421 (2003).